

(Chelating diphosphine)rhodium-Catalyzed Deuterioformylation of 1-Hexene: Control of Regiochemistry by the Kinetic Ratio of Alkylrhodium Species Formed by Hydride Addition to Complexed Alkene

Charles P. Casey* and Lori M. Petrovich

Contribution from the Department of Chemistry, University of Wisconsin, Madison, Wisconsin 53706

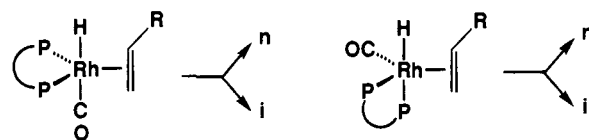
Received August 29, 1994[⊗]

Abstract: The deuterioformylation of 1-hexene catalyzed by (chelating diphosphine)rhodium catalysts gave nearly exclusive formation of $\text{CH}_3(\text{CH}_2)_3\text{CHDCH}_2\text{CDO}$ and $\text{CH}_3(\text{CH}_2)_3\text{CH}(\text{CH}_2\text{D})\text{CDO}$, with the deuterium label at the β -carbon and at the aldehyde carbon. Very little deuterium was incorporated into recovered hexenes. These results establish that the regiochemistry of aldehyde formation is set by a largely irreversible addition of a rhodium hydride to complexed 1-hexene to produce an alkylrhodium intermediate that is committed to aldehyde formation. Plausible steric explanations for the increased $n:i$ aldehyde regioselectivity seen for diequatorial chelates compared with apical–equatorial chelates are considered. However, such steric explanations are not supported by molecular mechanics calculations of probable transition states.

The very efficient homogeneous rhodium–phosphine catalysts for the industrially important hydroformylation reaction¹ were first developed by Wilkinson² and first employed by Union Carbide.³ Control of the regiochemistry of the hydroformylation of terminal alkenes remains a focus of industrial research. While extensive screening of a wide variety of phosphine and phosphite ligands has been reported, no detailed understanding of how phosphines control regiochemistry has emerged.

In Wilkinson's generally accepted dissociative mechanism for rhodium-catalyzed hydroformylation, regiochemistry is determined in the step that converts five-coordinate $\text{H}(\text{alkene})\text{-Rh}(\text{CO})\text{L}_2$ into either primary or secondary four-coordinate $(\text{alkyl})\text{Rh}(\text{CO})\text{L}_2$ (Scheme 1). The detailed structure of the key five-coordinate $\text{H}(\text{alkene})\text{Rh}(\text{CO})\text{L}_2$ intermediate is surely important in controlling the regiochemistry of hydroformylation, but this species has never been observed directly, presumably due to its high reactivity. However, Brown's NMR studies have shown that its precursor with $\text{L} = \text{PPh}_3$, $\text{HRh}(\text{CO})_2(\text{PPh}_3)_2$, is an 85:15 mixture of diequatorial and apical–equatorial isomers.⁴ At room temperature these isomers are in rapid equilibrium.

Since complexes with two equatorial phosphines might give very different regiochemistry than complexes with one equatorial and one apical phosphine ligand, we sought to study (chelating diphosphine)rhodium catalysts in which the natural bite angle of the diphosphine chelate would show a strong preference for one of the two geometries.



We employed the DIPHOS ligand (1,2-bis(diphenylphosphino)ethane), which has a natural bite angle of 84.5° , to favor the equatorial–apical geometry and the BISBI ligand (2,2'-bis((diphenylphosphino)methyl)-1,1'-biphenyl), which has a natural bite angle of 113° , to favor the equatorial–equatorial geometry. Two ligands with intermediate bite angles, T-BDCP (*trans*-1,2-bis((diphenylphosphino)methyl)cyclopropane) and DIOP (2,3-*O*-isopropylidene-2,3-dihydroxy-1,4-bis(diphenylphosphino)butane) were also employed. A surprisingly good linear correlation was observed between the percentage of n -aldehyde and the natural bite angle calculated by molecular mechanics (Chart 1).⁵

Before developing detailed explanations of the control of regiochemistry based on steric or electronic differences between diequatorial or apical–equatorial diphosphine complexes, we considered it crucial to test the assumption that the regiochemistry of aldehyde formation was controlled by an irreversible addition of rhodium hydride to a complexed alkene to give rhodium n -alkyl and i -alkyl complexes that were committed to aldehyde formation. The alternative that rhodium hydride addition to a complexed alkene might be fast and reversible deserves very serious consideration, since such processes are common in organometallic chemistry.⁶ In this alternative case, the regiochemistry of hydroformylation would depend upon the equilibrium ratio of rhodium n -alkyl and i -alkyl species and upon the relative rates of carbonylation of these two alkyl intermediates.

[⊗] Abstract published in *Advance ACS Abstracts*, May 1, 1995.

(1) (a) Parshall, G. W. *Homogeneous Catalysis: The Applications and Chemistry of Catalysis by Soluble Transition Metal Complexes*; Wiley: New York, 1980. (b) Tkatchenko, I. In *Comprehensive Organometallic Chemistry*; Wilkinson, G., Stone, F. G. A., Abel, E. W., Eds.; Pergamon: Oxford, U.K., 1982; Vol. 8, p 101. (c) Tolman, C. A.; Faller, J. W. In *Homogeneous Catalysis with Metal Phosphine Complexes*; Pignolet, L. H., Ed.; Plenum: New York, 1983; pp 81–109. (d) Wender, I.; Pino, P. In *Organic Syntheses via Metal Carbonyls*; Wiley-Interscience: New York, 1977; Vol. 2, pp 136–197.

(2) (a) Evans, D.; Yagupsky, G.; Wilkinson, G. *J. Chem. Soc. A* **1968**, 3133. (b) Yagupsky, G.; Brown, C. K.; Wilkinson, G. *J. Chem. Soc. A* **1970**, 1392. (c) Brown, C. K.; Wilkinson, G. *J. Chem. Soc. A* **1970**, 2753.

(3) Pruett, R. L. *Ann. N.Y. Acad. Sci.* **1977**, *195*, 239.

(4) Brown, J. M.; Kent, A. G. *J. Chem. Soc., Perkin Trans 2* **1987**, 1597.

(5) Casey, C. P.; Whiteker, G. T.; Melville, M. G.; Petrovich, L. M.; Gavney, J. A., Jr.; Powell, D. R. *J. Am. Chem. Soc.* **1992**, *114*, 5535.

(6) (a) Cotton, F. A.; Wilkinson, G. *Advanced Inorganic Chemistry*, 5th ed.; Wiley: New York, 1988; pp 1213–1216. (b) Evans, J.; Schwartz, J.; Urquhart, P. W. *J. Organomet. Chem.* **1976**, *81*, C37. (c) Lau, K. S. Y.; Becker, Y. Huang, F.; Baenziger, N.; Stille, J. K. *J. Am. Chem. Soc.* **1974**, *99*, 5664. (d) Bennett, M. A.; Crisp, G. T. *Organometallics* **1986**, *5*, 1792. (e) Bennett, M. A.; Crisp, G. T. *Organometallics* **1986**, *5*, 1800.

Scheme 1

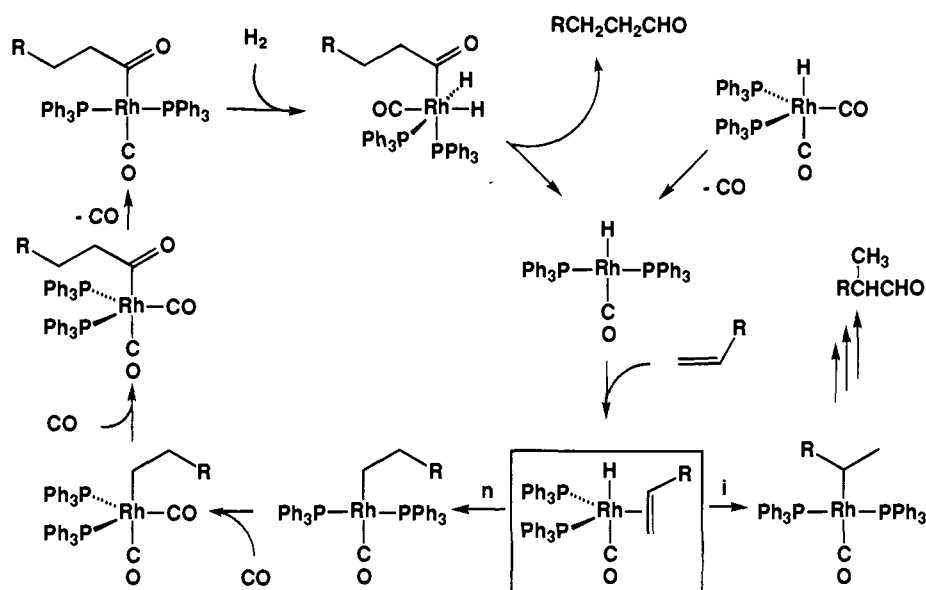


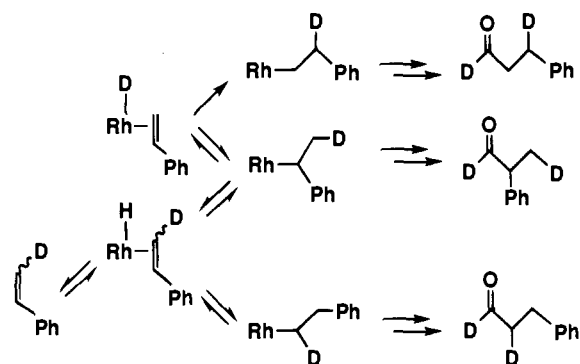
Chart 1

	BISBI	T-BDCP	DIOP	DIPHOS
Bite Angle	113°	107°	102°	85°
n : i	66	12	8.5	2.1

Deuterioformylation provides a sensitive means of distinguishing between these two modes of regiocontrol. If alkylrhodium formation is irreversible, then the aldehydes formed will have the deuterium label only on the aldehyde carbon and the β -carbon. Reversible alkylrhodium formation provides a way to place the deuterium label on the carbon α to the aldehyde carbonyl. If both alkylrhodium formation and alkene coordination are reversible, then deuterium would be incorporated into the recovered alkene.

Deuterioformylation has been used by Lazzaroni⁷ as a probe of reversible alkylrhodium formation in hydroformylation in the $\text{Rh}_4(\text{CO})_{12}$ -catalyzed deuterioformylation of styrene at 20 and 90 °C under 160 atm of 1:1 D_2 -CO. The mixture of alkenes recovered after 42% conversion at 90 °C consisted of 66% unlabeled styrene, 29% (*E*)- and (*Z*)- β -deuteriostyrene ($\text{PhCH}=\text{CHD}$), and 5% β,β -dideuteriostyrene ($\text{PhCH}=\text{CD}_2$); no α -deuteriostyrene was observed. We have calculated that approximately 32% of the total product consists of alkenes derived from reversible alkylrhodium formation. These results indicate that the rhodium *n*-alkyl intermediate proceeds directly to linear aldehyde but the rhodium branched benzylic intermediate is formed reversibly to give isomeric monodeuterated alkenes and rhodium hydride. In addition, these results require reversible coordination of styrene. When deuterioformylation was carried out at 20 °C, the mixture of alkenes recovered after 85% conversion consisted of 99% unlabeled styrene and only 1% (*E*)- and (*Z*)- β -deuteriostyrene. Thus at 20 °C, formation of both linear and branched alkylrhodium intermediates is largely irreversible.

Scheme 2



In a subsequent study, the aldehyde products obtained in the $\text{Rh}_4(\text{CO})_{12}$ -catalyzed deuterioformylation of styrene at 110 °C and 180 atm were examined.⁸ In addition to the β -deuterated aldehyde products $\text{PhCHDCH}_2\text{CDO}$ and $\text{PhCH}(\text{CH}_2\text{D})\text{CDO}$, expected from irreversible alkylrhodium formation, 10% of the α -deuterated linear aldehyde $\text{PhCH}_2\text{CHDCDO}$ was observed, but no α -deuterated branched aldehyde was seen. These results again suggest that rhodium *n*-alkyl formation is irreversible but that the rhodium branched benzylic intermediate is formed reversibly. Our detailed analysis of these results indicates that 57% of the deuterated products from deuterioformylation of styrene at 110 °C arise from reversible formation of a rhodium branched benzylic intermediate (Scheme 2).

While the rhodium-catalyzed deuterioformylation of styrene has been well studied, styrene is a rather unusual hydroformyl-

(7) (a) Lazzaroni, R.; Settambolo, R.; Raffaelli, A.; Pucci, S.; Vitulli, G. *J. Organomet. Chem.* **1988**, 339, 357. (b) Lazzaroni, R.; Raffaelli, A.; Settambolo, R.; Bertozzi, S.; Vitulli, G. *J. Mol. Catal.* **1989**, 50, 1.

(8) Uccello-Barretta, G.; Lazzaroni, R.; Settambolo, R.; Salvadori, P. *J. Organomet. Chem.* **1991**, 417, 111.

ation substrate that gives a much higher fraction of branched aldehyde compared with aliphatic alkenes. π -Benzyl complexes derived from styrene have been suggested as possible intermediates in the catalytic cycle to explain the larger amounts of branched products formed.^{1c,9} In contrast, deuterioformylation has been employed much less extensively to probe the rearrangement of alkylrhodium intermediates in the hydroformylation of aliphatic alkenes.^{10,11} Lazzaroni¹² investigated the Rh₄(CO)₁₂-catalyzed deuterioformylation of 1-hexene as a function of temperature and pressure but examined the deuterium label only in the recovered 1-hexene. At 20 °C, no incorporation of deuterium into recovered 1-hexene was observed. This was interpreted in terms of irreversible formation of alkylrhodium intermediates, but this conclusion is valid only if alkene coordination is rapidly reversible. At 100 °C, some incorporation of deuterium into recovered 1-hexene was observed. The results are consistent with 8% of the total product resulting from reversible (linear alkyl)rhodium formation and 25% from reversible (branched alkyl)rhodium formation. However, these studies provide only a fragmentary picture of the fate of deuterium, since product aldehydes were not investigated.

In general, these mechanistic studies of rhodium-catalyzed deuterioformylation indicate that alkylrhodium formation is nonreversible under mild conditions and reversible at higher temperatures. Yet, few details concerning the reversible nature of rhodium hydride addition in phosphine-modified hydroformylation are available.¹¹

Here we report the deuterioformylation of 1-hexene using the aforementioned series of bidentate chelating diphosphines with varying natural bite angles. Detailed analysis of both the deuterium-labeled aldehyde products and recovered 1-hexene show that >90% of the products are derived from irreversible formation of alkylrhodium intermediates. In addition, possible steric explanations for the higher *n:i* aldehyde regioselectivity seen for diequatorial chelates compared with that for apical-equatorial chelates are considered and discarded.

Results

Deuterioformylation of 1-Hexene. Deuterioformylation of 2.2 M solutions of 1-hexene in benzene was carried out at 32 °C under 6 atm of 52:48 D₂-CO using 3 mM 1:1 Rh-diphosphine or 1:2 Rh-monophosphine catalyst. Catalysts were prepared *in situ* from (acac)Rh(CO)₂ and phosphine ligands^{13,14} under a 52:48 D₂-CO atmosphere.

The production of heptanal and 2-methylhexanal was monitored by gas chromatography. The deuterioformylations were terminated after 40–50% conversion or 300 turnovers. The turnover rate and *n:i* selectivity for rhodium-catalyzed deuterioformylation of 1-hexene in the presence of BISBI, T-BDCP, DIPHOS, and triphenylphosphine are shown in Table 1. Turnover rates and ratios of heptanal to 2-methylhexanal were relatively constant throughout the deuterioformylation. Deu-

Table 1. Deuterioformylation and Hydroformylation of 1-Hexene with Rhodium-Phosphine Catalysts

phosphine	deuterioformylation			hydroformylation	
	% conversion	turnover rate ^a	<i>n:i</i> ^b	turnover rate ^a	<i>n:i</i> ^b
BISBI	44	13.2	66 ± 2	12.4	65.5 ^c
T-BDCP	41	3.5	13 ± 1	3.7	12.1 ^c
DIPHOS	41	1.2	2.0 ± 0.2	1.1	2.1 ^c
PPh ₃	51	13.6	3.6 ± 0.1	12.3	3.2

^a Turnover rate = (mol of aldehyde) (mol of Rh)⁻¹ h⁻¹. ^b *n:i* = (mol of heptanal):(mol of 2-methylhexanal). ^c Diphosphine hydroformylation turnover rates and *n:i* selectivities.¹²

Table 2. Deuterium Content of Heptanal and 2-Methylhexanal from Rhodium-Catalyzed Deuterioformylation of 1-Hexene in the Presence of Phosphine Ligands

Ligand	$\text{CH}_3-\text{CH}_2-\text{CH}_2-\text{CH}_2-\text{CH}_2-\text{CH}_2-\overset{\text{O}}{\parallel}{\text{C}}-\text{H}$						
	CH ₃	CH ₂	CH ₂	CH ₂	CH ₂	CH ₂	CHO
BISBI	-- ^a	--	--	0.98	0.02	1.00 ^b	
T-BDCP	--	--	--	1.00	--	1.00	
DIPHOS	--	--	--	0.99	--	1.00	
PPh ₃	--	--	--	1.00	--	1.00	
Ligand	$\text{CH}_3-\text{CH}_2-\text{CH}_2-\text{HCH} \quad \text{CH}_3 \quad \text{CH}-\overset{\text{O}}{\parallel}{\text{C}}-\text{H}$						
	CH ₃	CH ₂	CH ₂	HCH	CH ₃	CH	CHO
BISBI	-- ^a	--	--	0.97	0.02	1.00 ^b	
T-BDCP	--	--	--	0.98	--	1.00	
DIPHOS	--	--	--	0.95	--	1.00	
PPh ₃	--	--	--	0.98	--	1.00	

^a <0.01 deuterium based upon spectral signal to noise. ^b Integration value set at 1.0 deuterium.

terioformylation rates and selectivities were similar to those we previously reported for hydroformylation.⁵ The formation of byproducts such as 2-hexene, 2-ethylpentanal, heptanols, or aldol condensation products could not be detected by gas chromatography and are estimated to comprise <1% of the reaction mixture. Hexane-*d*₂ was detected by ²H NMR spectroscopy of the recovered 1-hexene fraction and is estimated to comprise ~1% of the reaction mixture.

Deuterium Distribution in Heptanal and 2-Methylhexanal. Pure samples of heptanal and 2-methylhexanal were obtained by distillation followed by preparative gas chromatography of an aldehyde-enriched fraction. The deuterium distribution in heptanal and 2-methylhexanal recovered from deuterioformylation experiments was accurately determined by ¹H and ²H NMR analysis. Since the error associated with the integration of the ¹H NMR spectrum is relatively large (estimated at 3–5%), small amounts of deuterium label α to the formyl group of the aldehydes could not be accurately determined using ¹H NMR. However, direct observation of deuterium label by ²H NMR spectroscopy gave an accurate measure of low levels of deuterium incorporation at the position α to the formyl group of the aldehydes. Table 2 shows the deuterium content corresponding to the different signals in heptanal and 2-methylhexanal in benzene.

The data in Table 2 clearly demonstrate that rhodium-catalyzed deuterioformylation in the presence of all the ligands investigated produces aldehydes in which the deuterium label

(9) Tanaka, M.; Watanabe, Y.; Mitsudo, T.; Takegami, Y. *Bull. Chem. Soc. Jpn.* **1974**, *47*, 1698.

(10) (a) Consiglio, G.; von Bezard, D. A.; Morandini, F.; Pino, P. *Helv. Chim. Acta* **1978**, *61*, 1703. (b) Pino, P. *J. Organomet. Chem.* **1980**, *7*, 431. (c) von Bezard, D. A.; Consiglio, G.; Morandini, F.; Pino, P. *J. Mol. Catal.* **1980**, *7*, 431. (d) Consiglio, G. *Organometallics* **1988**, *7*, 778. (e) Stefani, A.; Consiglio, G.; Botteghi, C.; Pino, P. *J. Am. Chem. Soc.* **1977**, *99*, 1058.

(11) (a) Stefani, A.; Consiglio, G.; Botteghi, C.; Pino, P. *J. Am. Chem. Soc.* **1973**, *95*, 6504. (b) Jongmsa, T.; Challa, G.; van Leeuwen, P. W. N. *M. J. Organomet. Chem.* **1991**, *421*, 121.

(12) Lazzaroni, R.; Uccello-Barretta, G.; Benetti, M. *Organometallics* **1989**, *8*, 2323.

(13) Trzeciak, A. M.; Ziolkowski, J. *J. J. Mol. Catal.* **1988**, *48*, 319.

(14) This system was first employed at Union Carbide: Pruet, R. L.; Smith, J. A. U.S. Patent 3,527,809.

Table 3. Deuterium Content of 1-Hexene Recovered from Rhodium-Catalyzed Deuterioformylation in the Presence of Phosphine Ligands Expressed as Multiples of Deuterium Natural Abundance (% Deuteration)

ligand	CH ₂ =CHD(CH ₂) ₃ CH ₃	<i>cis</i> - and <i>trans</i> -CHD=CH ₂ (CH ₂) ₃ CH ₃
BISBI	133 (2.0)	128 (1.9)
T-BDCP	4.5 (0.07)	4.4 (0.07)
DIPHOS	6.5 (0.10)	5.5 (0.08)
PPh ₃	12.4 (0.19)	3.6 (0.05)

is incorporated almost exclusively in the formyl group and the position β to the formyl group. Only when BISBI was used as the modifying ligand during deuterioformylation was a detectable amount of deuterium label (2%) found at the position α to the formyl group in both heptanal and 2-methylhexanal.

Deuterium Content and Distribution in Recovered 1-Hexene. Samples of unconverted 1-hexene were recovered from the deuterioformylations by preparative gas chromatography of a distillate enriched in 1-hexene. Deuterium content was determined by ²H NMR analysis of a known concentration of 1-hexene in a stock NMR solution of 0.270 M CDCl₃ in CCl₄. Only the vinyl resonances of 1-hexene showed deuterium enrichment. Table 3 lists the deuterium content of 1-hexene recovered from deuterioformylations as multiples of deuterium natural abundance and as percent deuteration (percent deuterated 1-hexene = (deuterated 1-hexene/(all deuterated aldehydes and hexenes)) \times 100). These data indicate very little deuterium incorporation in the recovered 1-hexene. Deuterioformylation in the presence of BISBI gave the highest deuterium content in the β -olefinic position at 133 \times natural abundance. At 44% conversion, 8.74 mmol of aldehyde and 0.43 mmol of deuterated alkene had formed. In comparison to the total amount of labeled products produced, deuterated 1-hexenes account for only 5% of the total product.

Discussion

The percentages of all deuterated species formed in the deuterioformylation of 1-hexene were calculated using data on percent conversion, the ratio of heptanal to 2-methylhexanal, and deuterium contents of aldehydes and recovered 1-hexene. Figure 1 is a graphic summary of these results; the boxes above the Rh-alkene-hydride species give estimates of the percentage of the reaction mixture that passes through these intermediates; the boxes below the Rh alkyl species give estimates of the amount of material passing irreversibly through the Rh alkyl to aldehyde. Table 4 shows that, for each phosphine-modified deuterioformylation, the amount of aldehyde recovered with the label in the β and formyl positions accounts for >90% of all deuterated materials. Table 5 summarizes data on the kinetic selectivity of alkylrhodium formation and the net regioselectivity of hydroformylation.

The regiochemistry of the deuterioformylation of 1-hexene in the presence of T-BDCP, DIPHOS, and PPh₃ is set by irreversible Rh-D addition to the alkene. For these three ligand systems, the only detectable materials derived from reversible formation of an alkylrhodium intermediate were very small amounts of CHD=CHC₄H₉ and CH₂=CDC₄H₉ (0.04–0.10%).

The control of the regiochemistry of deuterioformylation in the presence of BISBI is more complicated. Deuterioformylation gave measurable amounts of CHD=CHC₄H₉ and CH₂=CDC₄H₉ (2.3 and 2.4%) and measurable amounts of α -deuterated heptanal and 2-methylhexanal (1.9 and 0.03%). Detailed dissection of the BISBI labeling results shows that the initial ratio of *n*-alkyl to *i*-alkyl rhodium intermediates formed is 17:1 (94.3%:5.6%). The (*n*-alkyl)rhodium intermediate partitions between conversion to C₄H₉CHDCH₂CDO and reversal to CH₂=CDC₄H₉ in a 38:1 ratio (91.9 and 2.4%). Thus, the (*n*-alkyl)rhodium intermediate is largely converted directly to aldehyde. The small amount of (*i*-alkyl)rhodium intermediate (5.6%) partitions between conversion to 1.4% C₄H₉CH-

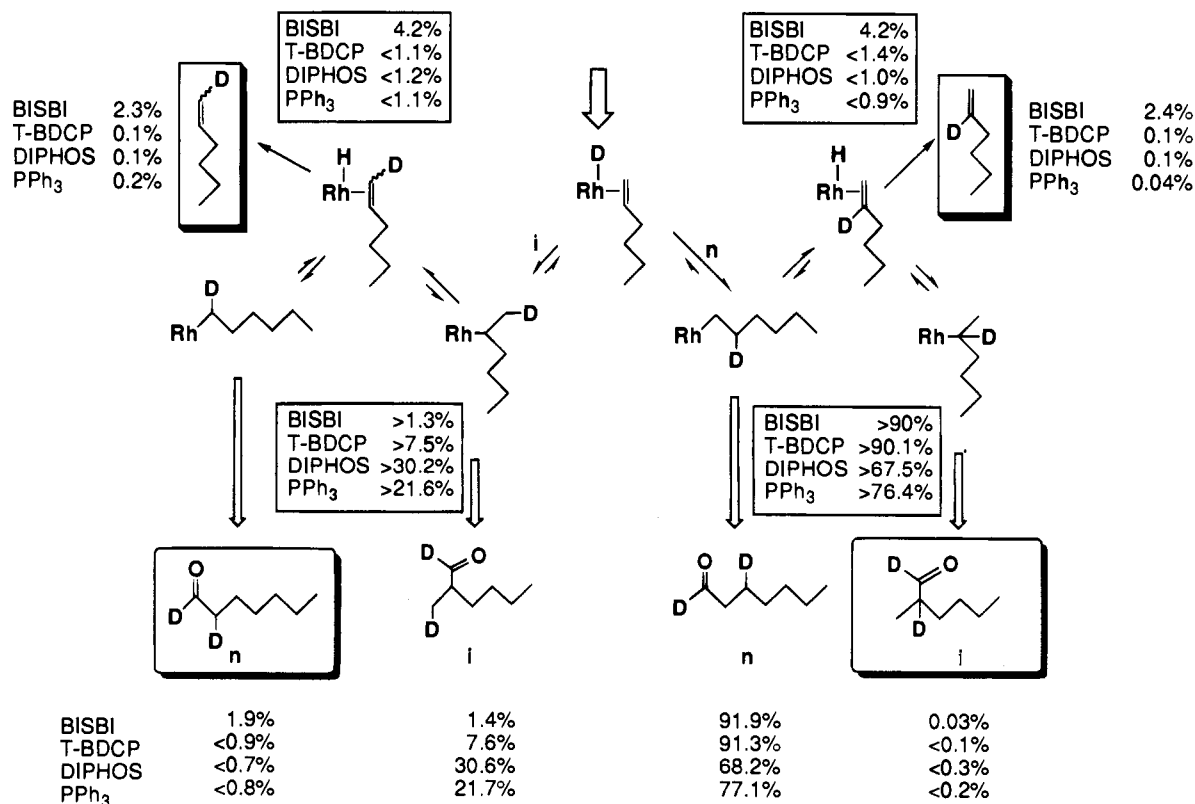


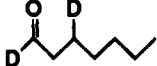

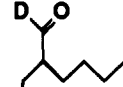
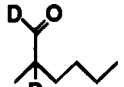
**Figure 1.** Deuterioformylation probe for reversibility of alkylrhodium formation in the presence of phosphine ligands.

Table 4. Percentage of Deuterated Products from Rhodium-Catalyzed Deuterioformylation in the Presence of Phosphine Ligands

Ligand	Percentage of Deuterated Species Present					
						
BISBI	2.3	2.4	91.9	1.9	1.4	0.03
T-BDCP	0.07	0.07	91.3	<0.9 ^a	7.6	<0.07 ^a
DIPHOS	0.1	0.1	68.2	<0.7	30.6	<0.3
PPh ₃	0.04	0.2	77.1	<0.8	21.7	<0.2

^a Maximum amount that may be present based upon signal to noise ratio in NMR.

Table 5. Kinetic Ratio of Alkylrhodium Intermediates and Observed *n:i* Regioselectivity

ligand	% linear alkylrhodium formation			% branched alkylrhodium formation			<i>n:i</i> selectivity	
	initial	reversible	net	initial	reversible	net	kinetic	observed
BISBI	94.3	2.4	91.9	5.6	4.2	1.4	17	66
T-BDCP	91.3		91.3	7.6		7.6	12	12
DIPHOS	68.2		68.2	30.6		30.6	2.2	2.2
PPh ₃	77.1		77.1	21.7		21.7	3.5	3.5

(CH₂D)CDO, 2.3% *cis*- and *trans*-CHD=CH(CH₂)₃CH₃, and 1.9% C₄H₉CH₂CHDCDO. Thus, 75% of the (*i*-alkyl)rhodium intermediate reverts to a 1-hexene complex (2.3 + 1.9%) and only 25% is converted directly on to branched aldehyde (1.4%). The observed regioselectivity of hydroformylation of 66:1 actually exceeds the kinetic 17:1 ratio of *n*-alkyl to *i*-alkyl rhodium intermediates since the *n*-alkyl intermediate is converted directly to aldehyde but the *i*-alkyl intermediate reverts to an alkene complex 75% of the time.

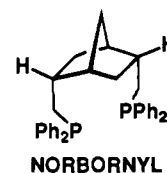
As mentioned earlier, a greater degree of reversibility of (*i*-alkyl)rhodium species compared with (*n*-alkyl)rhodium species was also seen by Lazzaroni in the Rh₄(CO)₁₂-catalyzed deuterioformylation of 1-hexene at 100 °C.¹²

Our results indicate that the final *n:i* aldehyde selectivity is largely set by the conversion of a five-coordinate H(alkene)-Rh(CO)L₂ complex to a four-coordinate (alkyl)Rh(CO)L₂ species. The dependence of this selectivity on the natural bite angle and chelation mode of diphosphines is striking. BISBI, which gives a high *n:i* selectivity of 66:1, chelates exclusively to diequatorial sites in five-coordinate rhodium and related iridium complexes.⁵ DIPHOS, which gives a low *n:i* selectivity of 2.1:1, spans an apical and an equatorial site in (DIPHOS)Ir(CO)₂H and (DIPHOS)Ir(PPh₃)(CO)H.¹⁵ T-BDCP, which gives intermediate *n:i* selectivity of 12:1, can bind as either a diequatorial or apical–equatorial chelate; low-temperature NMR showed that (T-BDCP)Ir(CO)₂H exists as a 3:1 mixture of apical–equatorial and diequatorial chelates.¹⁵ Brown's NMR studies showed that (PPh₃)₂Rh(CO)₂H exists as an 85:15 diequatorial to apical–equatorial mixture of isomers;⁴ under our conditions, PPh₃ gives an *n:i* selectivity of 3.2:1.

The correlation between regioselectivity and chelation mode requires that diequatorial diphosphines such as BISBI and equatorial–apical chelating diphosphines such as DIPHOS behave very differently. In developing explanations of the regiochemistry of hydroformylation, we have assumed that the diphosphines remain chelated throughout the catalytic cycle and particularly in the irreversible rhodium hydride addition step

that sets the regiochemistry. A reviewer suggested the alternative that while BISBI remains chelated, a significant fraction of the products resulting from DIPHOS catalyst might be derived from a monodentate complex. The possibility that the reactions of any chelated complex might result from low concentrations of a monodentate species is nearly impossible to rigorously exclude.

However, several considerations suggest that both DIPHOS and BISBI remain chelated throughout the hydroformylation catalytic cycle. Our molecular mechanics calculation of the increase in steric energy of DIPHOS upon chelation (2.9 kcal) is very similar to that for BISBI (2.1 kcal); therefore, there seems to be no steric reason that DIPHOS should chelate less well than BISBI.¹⁵ The norbornyl diphosphine ligand was calculated to have a large 12.2 kcal increase in steric energy upon chelation. Consistent with this strain of chelation, we have been unable to isolate any monomeric complexes of norbornyl and we believe that it does not act as a chelating ligand. Hydroformylation with norbornyl, which probably proceeds via a mixture of monophosphine and nonchelated diphosphine complexes, proceeds more than 8 times faster than hydroformylation with DIPHOS and produces a higher *n:i* ratio of aldehydes compared with DIPHOS (2.9 vs 2.1).⁵ Since DIPHOS and norbornyl have such different rates and regiochemistries of hydroformylation, it is likely that the catalysts differ structurally. This is consistent with DIPHOS acting as a chelate, while norbornyl does not.

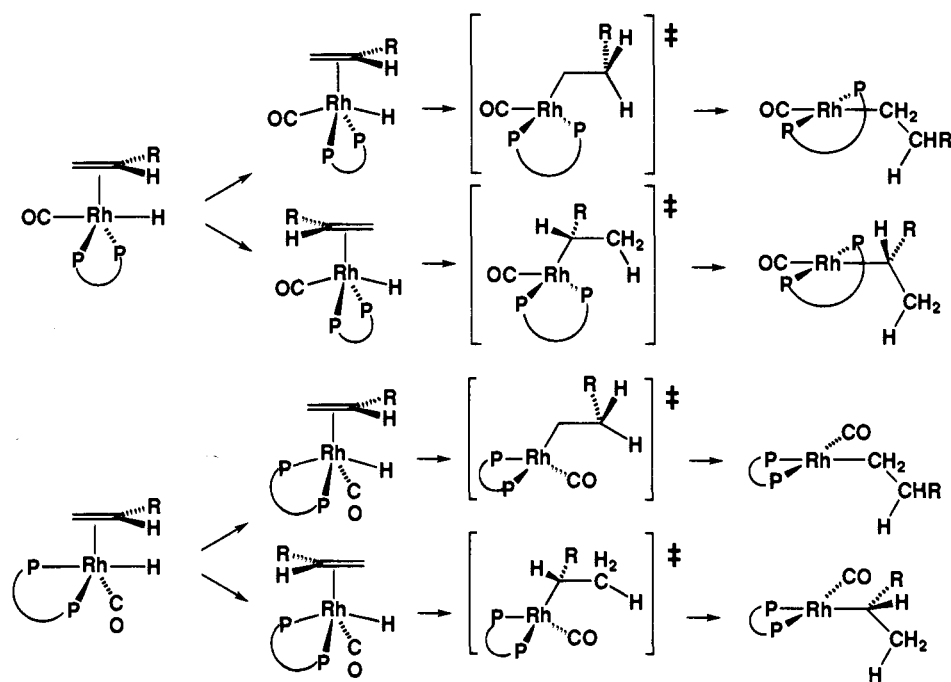


The correlation between regioselectivity and chelation mode suggests that diequatorial diphosphines such as BISBI and equatorial–apical chelating diphosphines such as DIPHOS have significantly different steric or electronic properties. We first considered the steric differences between diequatorial and

(15) Casey, C. P.; Petrovich, L. M. Unpublished results.

(16) Orpen, A. G.; Brammer, L.; Allen, F. H.; Kennard, O.; Watson, D. G.; Taylor, R. *J. Chem. Soc., Dalton Trans.* **1989**, S1.

Scheme 3



apical–equatorial chelates as a possible explanation for regioselectivity and outline our hypothesis below. In particular, we looked for a special role for flexible wide bite angle diphosphines in promoting formation of linear products. The explanation which we concocted on the basis of an examination of Dreiding molecular models is summarized in Scheme 3.

Our picture for the formation of rhodium alkyls begins with a trigonal-bipyramidal rhodium–hydride–alkene complex having an apical hydride ligand and an equatorial alkene whose C=C bond lies in the same plane as the rhodium–hydride bond. As the hydride begins to transfer to the β -carbon of the complexed alkene, the angle between the apical ligand initially trans to hydride and the forming alkyl–rhodium bond expands toward the 180° angle in the square-planar rhodium alkyl intermediate. Simultaneously, the angle between the equatorial ligands expands toward the 180° angle in a square-planar rhodium alkyl intermediate. This expansion of the diequatorial angle from 120 to 180° poses a potential problem for diequatorial chelating diphosphines such as BISBI, but our calculations suggest that BISBI can expand to 150° with only a small energetic penalty and the alkyl intermediate might be intercepted by CO before this angle expands fully to 180° .

For wide bite angle diphosphines such as BISBI, the chelating diphosphine occupies diequatorial sites. Examination of molecular models indicated no obvious steric problems for formation of the (*n*-alkyl)rhodium intermediate. However, for formation of the (*i*-alkyl)rhodium intermediate, models showed that the alkyl substituent of the terminal alkene would be held over a sterically large equatorial diphenylphosphine group. Such an interaction is present no matter which alkene enantioface coordinates to rhodium. This analysis suggests that (*n*-alkyl)rhodium formation would be substantially favored over (*i*-alkyl)rhodium formation.

For 90° chelating diphosphines such as DIPHOS, the chelating diphosphine initially spans an equatorial and an apical position. For formation of an (*n*-alkyl)rhodium intermediate no steric problems were apparent from inspection of models. For formation of an *i*-alkyl intermediate, complexation of one alkene enantioface led to unfavorable steric interactions for the alkyl substituent of the terminal alkene held over a sterically

large equatorial diphenylphosphine group. This interaction was similar to that for diequatorial chelates. However, complexation of the opposite alkene enantioface places the alkyl substituent of the terminal alkene over a sterically small equatorial CO ligand. This suggested that (*i*-alkyl)rhodium formation could occur more readily for apical–equatorial diphosphine than for diequatorial diphosphine ligands because there is always a sterically feasible pathway to *i*-alkyl products.

While this examination of molecular models gave a seductively facile explanation for the greater *n*:*i* regioselectivity seen for flexible wide bite angle diphosphines, our ability to read nonexistent differential steric effects into examination of molecular models cannot be overestimated. To obtain a more objective and semiquantitative estimate of steric effects in these systems, we turned to molecular mechanics calculations of models for transition-state geometries to see if the steric effects seen on examination of models would be supported or negated by molecular mechanics calculations.

The transition-state geometry chosen for molecular mechanics calculations was halfway along a symmetric reaction coordinate between the starting trigonal-bipyramidal (diphosphine)Rh(propylene)(CO)H complex and the product square-planar (diphosphine)Rh(*n*-propyl)(CO) and (diphosphine)Rh(isopropyl)(CO) intermediates. For efficient transfer of hydride to the alkene, the axial L–Rh–H system and the equatorial alkene C=C were restricted to the same plane. The angle between the two remaining equatorial ligands was set at 150° , the midpoint between the 120° angle of the starting rhodium–alkene–hydride complex and the 180° angle of the square-planar alkyrhodium intermediate (for BISBI then, the P–Rh–P angle is set at 150°). The angles between the axial ligand and the two equatorial ligands were set at 90° , since that is the angle in both the starting material and the intermediate (for DIPHOS then, the P–Rh–P angle is set at 90°). The Rh–C_{alkene}–C_{alkene} angle was set at 90° , halfway between the 70° angle of the starting rhodium–alkene–hydride complex and the 109.5° angle of the planar intermediate. The Rh–C distance used in calculations was 2.15, the midpoint between the Rh–C(sp²) bond distance of Rh–alkene complexes and the Rh–C(sp³)

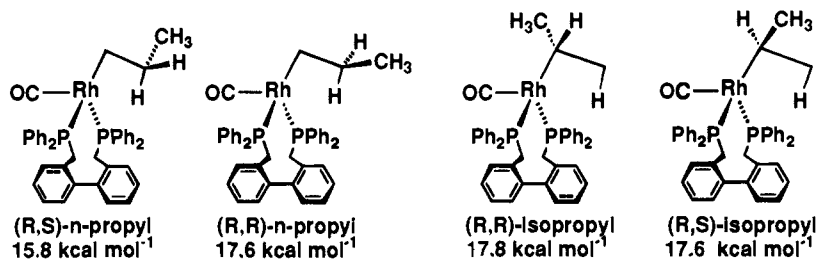


Figure 2. Calculated energies of (BISBI)Rh(*n*-propyl)(CO) and (BISBI)Rh(isopropyl)(CO) transition-state models.

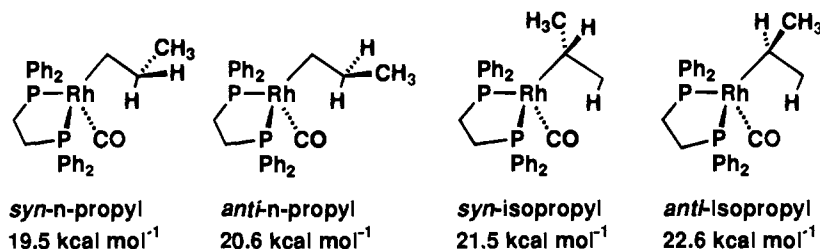
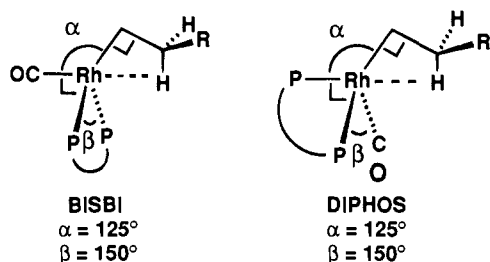


Figure 3. Calculated energies of (DIPHOS)Rh(*n*-propyl)(CO) and (DIPHOS)Rh(*i*-propyl)(CO) transition-state models.

bond distance of alkylrhodium complexes.¹⁴ The transition-state models for BISBI and DIPHOS are shown:



The relative steric energies of the (BISBI)Rh(*n*-propyl)(CO) and (BISBI)Rh(isopropyl)(CO) transition-state models calculated by molecular mechanics are shown in Figure 2. The energy difference between the lowest energy (BISBI)Rh(*n*-propyl)(CO) model (15.8 kcal mol⁻¹) and the lowest energy (BISBI)Rh(isopropyl)(CO) model (17.6 kcal mol⁻¹) is 1.9 kcal mol⁻¹. This value is very close to the 1.7 kcal mol⁻¹ required for the 17:1 partitioning between (*n*-propyl)- and (isopropyl)rhodium intermediates deduced from the deuterioformylation studies with BISBI. (The 66:1 *n*:*i* aldehyde selectivity observed in hydroformylation with BISBI corresponds to 2.5 kcal mol⁻¹.)

Similarly, the relative steric energies of the (DIPHOS)Rh(*n*-propyl)(CO) and (DIPHOS)Rh(isopropyl)(CO) transition-state models were calculated by molecular mechanics (Figure 3). The energy difference between the lowest energy (DIPHOS)Rh(*n*-propyl)(CO) model (19.5 kcal mol⁻¹) and the lowest energy (DIPHOS)Rh(isopropyl)(CO) model (21.5 kcal mol⁻¹) is 2.1 kcal mol⁻¹. This value is substantially higher than the 0.5 kcal mol⁻¹ required for the 2.1:1 *n*:*i* aldehyde selectivity observed in hydroformylation with DIPHOS. More disturbing was the fact that these calculations suggested that DIPHOS ($\Delta\Delta G^\ddagger = 2.1$ kcal mol⁻¹) should be more selective for linear aldehyde than BISBI ($\Delta\Delta G^\ddagger = 1.9$ kcal mol⁻¹), when in fact the opposite trend was observed.

Clearly, molecular mechanics calculations for this transition state do not support a steric explanation for the greater *n*:*i* aldehyde selectivity of BISBI relative to DIPHOS. Systematic molecular mechanics calculations for other transition states along the reaction coordinate between the starting trigonal-bipyramidal (diphosphine)Rh(propylene)(CO)H complex and the product square-planar (diphosphine)Rh(*n*-propyl)(CO) and (diphosphine)Rh(isopropyl)(CO) intermediates were carried out by

varying the OC–Rh–C_{alkyl} angle between 70 and 180° at 10° intervals and varying the P–Rh–P angle between 120 and 180° at 10° intervals. However, these calculations also failed to explain the observed differences between the two ligands.

Since molecular mechanics fail to support a steric explanation for the much higher *n*:*i* aldehyde ratios observed from diequatorial chelates such as BISBI compared with apical–equatorial chelates such as DIPHOS, we must consider whether the electronic difference between diequatorial chelates and apical–equatorial chelates may be responsible for the differences in regioselectivity. Because the electronic interaction between two apical ligands or between two equatorial ligands is stronger than the interaction between apical and equatorial ligands, electronic differences can be expected between diequatorial chelated complexes and equatorial–apical chelated complexes. For example, back-bonding from rhodium to the alkene ligand in the equatorial plane would be expected to be stronger for the BISBI complex with two strong donor phosphines in the equatorial plane than for the DIPHOS complex with only a single donor phosphine in the equatorial plane. Also, the apical hydride of the BISBI complex is trans to a CO ligand and would be expected to be more acidic than the hydride of the DIPHOS complex, which is trans to a phosphine. We are currently trying to devise experiments to test the hypothesis that the greater regioselectivity seen for diequatorial chelating ligands such as BISBI may be due to an electronic difference between chelating modes.

Experimental Section

General Considerations. ¹H NMR spectra were measured on a Bruker AM500 spectrometer. ²H NMR spectra were obtained on a Bruker AM500 spectrometer operating at 76.8 MHz. Analytical-scale gas chromatography was performed on a Hewlett-Packard 5890A gas chromatograph connected to an HP3390A integrator. Preparative gas chromatography was performed on a Varian Aerograph Model 90-P gas chromatograph. Benzene, benzene-*d*₆, and toluene were distilled from purple solutions of sodium and benzophenone. 1-Hexene was distilled from sodium, stored under N₂, and used within 2 weeks of distillation.

All air-sensitive materials were handled using standard high-vacuum manifold and inert-atmosphere glovebox techniques. (acac)Rh(CO)₂¹⁷

(17) Varshavskii, Y. S.; Cherkasova, T. G. *Russ. J. Inorg. Chem.* **1967**, *12*, 899.

and T-BDCP¹⁸ were prepared by literature methods. PPh₃ and DIPHOS were purchased from Aldrich and recrystallized from EtOH prior to use. BISBI was obtained from Texas Eastman. Analyzed mixtures of 1:1 CO–H₂ and CO were obtained from Matheson Gas Products. D₂ was obtained from Cambridge Isotope Laboratories.

Preparation and Analysis of D₂–CO Mixture. A 52:48 D₂–CO mixture was obtained by adding roughly equal portions of D₂ and CO to a large evacuated cylinder and rolling the cylinder gently. The ratio of the gas mixture was determined using a Toepler pump system. A sample of the gas mixture was circulated on the Toepler pump system through a loop containing solid CuO at 300 °C to oxidize CO to CO₂ and D₂ to D₂O. The oxidized mixture (771 μmol) contained 373 μmol of gas that passed through a trap at –78 °C and 7 μmol of gas that passed through a trap at –190 °C. This indicated the presence of 398 μmol of D₂O and 366 μmol of CO₂ (52:48).

Catalytic Deuterioformylation of 1-Hexene. Deuterioformylation reactions were performed in a 90-mL Fischer–Porter bottle equipped with a gas inlet valve, a liquid sampling valve equipped with septa, and a star-head magnetic stirbar. A magnetic stirrer placed below the bath provided efficient stirring. The pressure apparatus was immersed in a constant-temperature bath maintained at 33.6 ± 0.5 °C in a well-ventilated fume hood.

(acac)Rh(CO)₂ (7.9 mg, 0.031 mmol) and a chelating diphosphine (0.031 mmol for diphosphines, 0.062 mmol for monophosphines) were placed in the pressure apparatus under N₂ in a glovebox. The system was flushed with 70 psig of D₂–CO three times and then pressurized to 70 psig with 52:48 D₂–CO. Benzene (6.0 mL) and toluene (internal GC standard, 0.20 mL, 1.9 mmol) were added by gastight syringe to the pressurized system through the septa of the liquid sampling valve. After 1 h of stirring, 1-hexene (2.50 mL, 20 mmol) was added by gastight syringe. The pressure of the system was maintained throughout the reaction at 70 ± 2 psig (5.8 atm) by adding additional D₂–CO periodically. Samples were removed for analysis every 35–50 turnovers (3–12 h depending on the ligand) via gastight syringe. Heptanal and 2-methylhexanal were analyzed by temperature-programmed gas chromatography on an HP5890A chromatograph interfaced to an HP3390A integrator using a 10 m × 0.53 mm methyl silicone capillary column.

Catalytic Hydroformylation of 1-Hexene. Hydroformylation reactions were performed in the same manner as deuterioformylation reactions using analyzed CO–H₂ (50.02% CO, 49.98% H₂). Hydroformylation data for BISBI-, T-BDCP-, and DIPHOS-modified reactions have been previously published.⁵

Recovery and Purification of 1-Hexene and Aldehydes. Upon termination of each deuterioformylation reaction, all volatiles were immediately vacuum-transferred from the rhodium catalyst. A crude vacuum distillation of the volatiles provided a 1-hexene-rich and an aldehyde-rich fraction. Pure samples of 1-hexene, heptanal, and 2-methylhexanal were obtained by preparative gas chromatography of these enriched fractions on a Varian Aerograph Model 90-P gas chromatograph using a 10 ft × 3/8 in. 25% Carbowax 20M on 60/80 Chromasorb W column.

NMR Analysis of Heptanal from Deuterioformylation. ¹H NMR (benzene-*d*₆, 60 s relaxation delay): δ 1.83 (d, *J* = 7 Hz, –CHDCH₂–CDO), 1.27 (m, –CH₂CHDCH₂–CDO), 1.15 (m, –CH₂CH₂CHDCH₂–CDO), 1.02 (m, CH₃(CH₂)₂CH₂CHDCH₂–CDO), 0.82 (t, *J* = 7 Hz, CH₃(CH₂)₃CHDCH₂–CDO). CH₃(CH₂)₄CHDCDO was not present in large enough concentration to distinguish ¹H NMR resonances. ²H NMR spectra (benzene, 20 s relaxation delay): δ 9.32 (bs, –CHDCH₂–CDO and –CH₂CHDCDO), 1.78 (bs, –CHDCDO), 1.23 (bm, –CH₂–CHDCH₂–CDO).

(18) Aviron-Violet, P.; Colleville, Y.; Varagnat, J. *J. Mol. Catal.* **1979**, 5, 41.

NMR Analysis of 2-Methylhexanal from Deuterioformylation. ¹H NMR (benzene-*d*₆, 60 s relaxation delay): δ 1.81 (m, –CH₂CH–(CH₂D)CDO), 1.35 (m, –CH₂CHHCH(CH₂D)CDO), 1.05 (m, CH₃–(CH₂)₂HCHCH(CH₂D)CDO), 0.78 (t, *J* = 7 Hz, CH₃CH₂), 0.77 (d, *J* = 7 Hz, –CH(CH₂D)CDO). CH₃(CH₂)₃CD(CH₃)CDO was not present in large enough concentration to distinguish ¹H NMR resonances. ²H NMR (benzene, 20 s relaxation delay): δ 9.27 (s, –CH(CH₂D)CDO and –CD(CH₃)CDO), 1.78 (s, –CH₂CD(CH₃)CDO), 0.72 (s, –CH–(CH₂D)CDO).

NMR Analysis of 1-Hexene Recovered from Deuterioformylation. ²H{¹H} NMR (CCl₄): δ 5.69 (s, CH₂=CD–), 4.90 (s, *trans*-CHD=CH–), 4.83 (s, *cis*-CHD=CH–). Due to the very small amount of deuterium incorporation, the average of two estimates of deuterium content was used. Integration of the deuterium-enriched signals was compared both to the signal for the external standard CDCl₃ and to the natural abundance of deuterium in the methylene signal of CH₂=CH–CH₂(CH₂)₂CH₃ at δ 1.94. The estimates of deuterium incorporation calculated using these two methods differed by less than a factor of 1.5.

Molecular mechanics calculations were performed in a manner similar to that used by us to calculate natural bite angles.¹⁹ An Evans and Sutherland PS300 graphics terminal was employed using the program MACROMODEL version 3.5 developed by Still.²⁰ Minimizations were performed using the Amber force field²¹ with additional force field parameters reported by Allinger²² for the calculation of tertiary phosphines plus several new force field parameters to constrain angles in the transition-state models. Bond stretches (bond, length (Å), force constant (kcal mol^{–1} Å^{–2}): Rh–P, 2.315, 201;²² Rh–CO, 1.895, 250;²³ Rh≡O, 1.128, 1115;²³ Rh–C_{alkyl}, 2.115, 250.^{24,25} The Rh–CH–CH₃ bond angle of the isopropyl complex was taken as 109.5° with a force constant of 40 kcal mol^{–1} rad^{–2}.²⁶ Nonbonded interactions with rhodium were modeled with a 2.00 Å radius for Rh and ε of 0.68 kcal mol^{–1}.⁵ The Rh–C_{alkyl}–C_{alkyl} bond angle involving the alkene C=C unit was constrained to 90° with a force constant of 5000 kcal mol^{–1} rad^{–2}. The Rh–C_{alkyl}–C_{alkyl}–H torsion angle was constrained to 180° with a torsional parameter of 1000 kcal mol^{–1}. For calculations of the BISBI complexes, the P–Rh–P (150°), P–Rh–C_{alkyl} (102.2°), P–Rh–CO (90°), and OC–Rh–C_{alkyl} (125°) angles were all constrained with a force constants of 5000 kcal mol^{–1} rad^{–2}, and the OC–Rh–C_{alkyl}–C_{alkyl} torsion angle was constrained to 180° with a torsional parameter of 1000 kcal mol^{–1}. For calculations of the DIPHOS complexes, the P_e–Rh–CO (150°), P_e–Rh–C_{alkyl} (102.2°), CO–Rh–C_{alkyl} (102.2°), P_e–Rh–P_a (90°), OC–Rh–P_a (90°), and P_a–Rh–C_{alkyl} (125°) angles were all constrained with force constants of 5000 kcal mol^{–1} rad^{–2}, and the P_a–Rh–C_{alkyl}–C_{alkyl} torsion angle was constrained to 180° with a torsional parameter of 1000 kcal mol^{–1}.

Acknowledgment. Financial support from the Department of Energy, Office of Basic Energy Sciences, is gratefully acknowledged. L.M.P. thanks the National Science Foundation for a predoctoral fellowship. We thank Dr. Paul Kiprof for help with the molecular mechanics calculations.

JA942880L

(19) Casey, C. P.; Whiteker, G. T. *Isr. J. Chem.* **1990**, 30, 299.
(20) Still, W. C. MacroModel V1.5; Department of Chemistry, Columbia University, New York, NY 10027.

(21) Weiner, P.; Kollman, P. J. *Comput. Chem.* **1981**, 2, 287.
(22) Bowen, J. P.; Allinger, M. L. *J. Org. Chem.* **1987**, 52, 2937.
(23) *Quanta Version 3.3 Parameter Handbook*; Molecular Simulations, Inc.: 200 Fifth Ave., Waltham, MA 02154.

(24) Default AMBER M–C stretching force constant.²¹
(25) Average of Rh–C(sp²) and Rh–C(sp³) bond distances.¹⁶
(26) AMBER C(sp³)–C(sp³)–C(sp³) bending force constant.²¹